

Article

Recovery of Apatite from Magnetic Concentration Tailings by Flotation

Luis Valderrama ^{1,*}, Osvaldo Gómez ² , Osvaldo Pavez ¹ and Mario Santander ¹

¹ Department of Metallurgy, Engineering Faculty, University of Atacama, Copiapó 1532297, Atacama Region, Chile; osvaldo.pavez@uda.cl (O.P.); mario.santander@uda.cl (M.S.)

² Minera del Pacífico Company, La Serena 1710151, Coquimbo Region, Chile

* Correspondence: luis.valderrama@uda.cl

Abstract: Iron concentration tailings contain many valuable minerals, including apatite, which is not currently being recovered despite its use to make fertilizers and chemicals. This article proposes a flotation circuit to recover apatite from tailings generated by mining in Chile, based on laboratory tests and using the “Split Factor” method. The iron tailings were characterized by granulometry, chemical and mineralogical analyses, zeta potential, and contact angle. The effect of the collector, frother, and dispersant dose, along with the number of flotation stages, on both the grade and recovery of P_2O_5 were studied. The results indicate that it is possible to produce concentrates with a P_2O_5 grade of 29.1% and 89.6% recovery in a flotation circuit that includes the rougher–scavenger–cleaner stages. To obtain these results, it is only necessary to condition the iron tailings with 400 gt^{-1} of Atrac-2600, 400 gt^{-1} of sodium silicate, 10 min of conditioning time, pH adjustment to 10, and a time for the rougher, cleaner, and scavenger stages set at 10, 7.6, and 6.8 min, respectively. A chemical interaction is suggested, where the collector is specifically adsorbed onto the apatite surface.

Keywords: apatite; zeta potential; tailing; Atrac-2600; flotation circuit



Citation: Valderrama, L.; Gómez, O.; Pavez, O.; Santander, M. Recovery of Apatite from Magnetic Concentration Tailings by Flotation. *Minerals* **2024**, *14*, 441. <https://doi.org/10.3390/min14050441>

Academic Editors: Rachid Hakkou, Mohamed Loutou, Yassine Taha and Cyril O'Connor

Received: 23 January 2024

Revised: 20 March 2024

Accepted: 26 March 2024

Published: 23 April 2024



Copyright: © 2024 by the authors. Licensee MDPI, Basel, Switzerland. This article is an open access article distributed under the terms and conditions of the Creative Commons Attribution (CC BY) license (<https://creativecommons.org/licenses/by/4.0/>).

1. Introduction

The world's production of phosphate rock in 2019 was 240 million tons. Phosphate ore is the only significant global resource of phosphorus, and it is found in marine sedimentary phosphorite deposits located in China, Africa, the Middle East, the United States, and in igneous deposits present in Brazil, Canada, Finland, Russia, and South Africa. Eighty percent of the world's phosphate supply comes from sedimentary deposits [1].

In Chile, the production of phosphate rock has been minimal. In 2019, only 3405 t were produced when these valuable resources were available. On the other hand, Chile imported 355,416 t phosphate fertilizers for agriculture in the same year [2].

The global demand for these raw materials has increased and will double in the coming years. With the increase in demand, ore grades have decreased, and the quality of the product required is higher, making the concentration process more complicated [3].

Tailings can be transformed into valuable secondary mining sources by combining mineral recovery with environmental management, eliminating the need for further size reduction, as the tailings have already been mined, crushed, and ground, and treatment costs are much lower compared to primary minerals. In Chile, copper tailings have a particle size of d_{80} of 90 μm , an appropriate size for flotation [4–6].

The iron reserves of Minera del Pacífico Company amount to approximately 7000 million tons with a grade exceeding 30% in total Fe. These reserves are located in the so-called Chilean Iron Belt, consisting of around 80 deposits of iron–apatite oxides. This belt of iron deposits stretches approximately 600 km along the Coastal Range, between the regions of Atacama and Coquimbo [7]. In this line, the tailings produced by the treatment of iron ores from the Cretaceous Iron Belt in the Mountain Range of northern Chile [8] are found,

which contain iron oxide–apatite (IOA) deposits. The concentration process produces a non-magnetic tailing containing apatite, with grades between 1–3% P₂O₅ [9].

Flotation is a method based on the difference in physicochemical properties between valuable minerals and gangue [10]. The wettability of the surface plays a decisive role in its buoyancy. The contact angle between the ore surface and the bubble is often used as an ore surface wettability-relevant indicator [11].

Flotation has been the most widely used technique when a minimum degree of P₂O₅ (28% to 35%) for fertilizer production is required. Similarly, the most common collectors used in phosphate flotation are fatty acids and their salts [12,13]. These collectors are employed to recover apatite in alkaline pH. However, the use of these collectors is only when their beneficiation is by the flotation of non-complex apatite minerals.

Under these conditions, the fatty acids become ionized. The carboxyl group reacts with the calcium ions present on the surface of the apatite and in the solution. This reaction produces non-soluble calcium carboxylate, which has Ca–O bonds. The Ca ions of the apatite surface interact with O atoms of the carbonyl group, forming the calcium carboxylate. This compound would precipitate at the mineral/solution interface, hydrophobizing the surface of the apatite due to the chemical bond that presents characteristics of precipitation of substances with low solubility [14].

Worldwide, tall oil is the principal source of fatty acids used in flotation plants, although, in recent years, alternative sources have appeared, such as rice, soybean, flaxseed, passion fruit, nut, jojoba, coconut, pequi, and grape [15–17].

In recent years, synthetic collectors have been developed as more sophisticated reagents when the fatty acids used to float complex phosphate minerals are not feasible due to their low selectivity and metallurgical recovery. In the case of magmatic apatite minerals, a practice that is becoming common is the mixing of synthetic collectors with fatty acids to increase the efficiency of the fatty acid. The disadvantage these collectors have is the high dose of reagents required for good performance [18].

Iron oxide–apatite (IOA) deposits are characterized by their magnetite–apatite–actinolite associations. These deposits may contain significant amounts of rare earth elements that can be exploited as by-products. They are high-grade mines in magnetite and variable concentrations of apatite, and these contain rare earth elements [19], which are processed to obtain iron concentrate. Reprocessing these tailings would have the advantage of partially recycling this material to produce a set of critical elements [20]. Apatites have different buoyancy in the flotation process, and this depends on the geological origin, whether it is of the igneous, sedimentary, or metamorphic type.

The circular economy and the utilization of secondary raw materials have gained increasing interest within the mining industry, and the critical raw material extraction from tailings can reduce waste materials and add more economic value to raw ore. Refs. [21,22] studied the flotation of apatite from iron tailings from IOA-type deposits. The processing of these tailings is a great challenge since the characteristics of the feed material can limit the possibility of an acceptable high grade in the final product and good recovery. Tailings with different phosphate contents from the magnetic separation process of magnetite have been studied for apatite recovery by flotation. With the results of the tailing beneficiation at the laboratory level and in the pilot plant using tall oil as a collector and sodium silicate as a dispersant in the flotation, an apatite concentrate is obtained with acceptable P₂O₅ grades for the manufacture of fertilizer. Additionally, the apatite concentrate also contains rare earth element concentrates.

Considering that phosphorus recovery could be carried out from tailings [23,24] to ensure the supply of phosphorus for fertilizers, the purposes of this work were as follows: (a) to characterize and evaluate the performance of a new synthetic collector, Atrac-2600 (anion collector sold by AkzoNobel-Brazil), to float apatite from iron tailings, different from fatty acid collectors, and (b) to design a laboratory-scale flotation circuit to produce apatite concentrate of commercial interest from the iron tailings generated in the Minera del Pacífico Company, located in the Atacama Region-Chile.

2. Materials and Methods

2.1. Preparation of the Sample

Pure samples of natural calcium phosphate crystals were obtained from the Los Molles mine of the Minera del Pacífico Company in Huasco, Atacama Region, Chile. These samples were reduced in size, and the apatite crystals with the lowest impurity contents were selected using an optical microscope. The sample was divided into quarters, with one portion used to make briquettes to determine the contact angle and the other was ground for zeta potential tests and chemical analysis.

The flotation tests were carried out using tailings obtained from the “El Trigo” deposit of the same company. The sample was dispersed and classified on a 210-micrometer opening sieve, where the retained fraction was removed. The fraction that passed was homogenized and divided into quarters. Then, representative samples were obtained for granulometric, chemical, and mineralogical characterization, and flotation tests at the laboratory level.

2.2. Flotation Tests, Zeta Potential, and Contact Angle Measurements with Pure Apatite

In the flotation tests of pure apatite, sodium hydroxide (NaOH) and sulfuric acid (H_2SO_4) were used as pH regulators, sodium silicate (Si-Na) as a dispersant, methyl isobutyl carbinol as a frother agent, and sodium oleate (O-Na) and Atrac-2600 as collectors. In previous research, the author demonstrated that the Atrac-2600 collector has better recovery and selectivity than sodium oleate [25].

The zeta potential of apatite was measured using the microelectrophoresis technique in the Zeta Meter System 4.0 equipment. To prepare the suspension, 0.01 g of apatite with a particle size smaller than 37 μm was added to 100 mL solution. The suspension was left to settle for 24 h to allow particles smaller than 5 μm to float. Potassium nitrate (KNO_3) was used as a supporting electrolyte at a concentration of $1 \times 10^{-3} \text{ mol}\cdot\text{L}^{-1}$ and $1 \times 10^{-5} \text{ mol L}^{-1}$. The pH values were adjusted using sodium hydroxide (NaOH) and hydrochloric acid (HCl). Tests were also performed using sodium oleate and Atrac-2600.

The contact angle was measured using the sessile drop method. The equipment used was a Ramé-Hart Model 190 CA goniometer. The apatite sample was immersed in three different liquids: deionized water, a solution prepared with sodium oleate, and another with Atrac-2600, and at different pH values (2, 4, 6, 8, 10, and 12) to measure the contact angle. The purified apatite mineral sample was mounted on an epoxy resin briquette, polished to a mirror surface, and then immersed in the quartz cell containing the test liquids. The cell was mounted on the goniometer slide, and then an air bubble was generated with the goniometer microsyringe and placed on the apatite surface. Finally, the contact angle was measured three times on both sides of the bubble.

2.3. Flotation Tests of Tailings Containing Apatite

The flotation tests were performed in a Denver D12 flotation cell subaeration of 2.5 L. In all flotation tests, the solids concentration was kept constant at 35% with a pH of 10, 1200 rpm, aeration rate of 10 L min^{-1} , and the conditioning and flotation time was 10 min. The mineralized froths were recovered by scraping the froth layer every 15 s and adding water to the test to maintain the suspension level periodically. The first flotation tests were performed to evaluate the type and dose of the collector and frother agent, keeping the dispersant constant based on the grade and recovery of P_2O_5 .

2.4. Kinetic Flotation Tests and Open Cycle Tests

Kinetic flotation tests were performed on the rougher, cleaner, and scavenger stages to determine the optimal flotation time. The experimental procedure applied in the flotation kinetics for each stage was identical. However, no reagents were added during the cleaner and scavenger flotation stages. The mineralized froths were removed at time intervals of 0–1, 1–3, 3–5, 5–7, and 7–10 min. Subsequently, the concentrates and tailings obtained were filtered, dried at 80 °C, weighed to recover the mass, and analyzed to establish the chemical

composition in all flotation tests. Open-cycle tests were performed after determining the optimal flotation times to calculate the split factors of the three flotation stages. These tests were performed using the optimal times established in the flotation kinetics.

3. Results

Table 1 presents the chemical composition of the tailing sample to be fed to the flotation tests. The chemical analyses were performed using the colorimetric technique for phosphorus, the potassium dichromate volumetric technique for iron, and atomic absorption spectroscopy for silica, aluminum, calcium, magnesium, and sodium.

Table 1. Chemical composition of the tailing sample.

Species	P ₂ O ₅	SiO ₂	Fe _T	Al ₂ O ₃	CaO	MgO	Na ₂ O
Composition, %	1.8	46.4	25.9	6.8	6.1	4.9	2.7

Table 2 presents the mineralogical analysis performed on the tailing sample. The different mineralogical species that form the samples can be observed, where 3.4% corresponds to apatite. The other mineralogical species contained in high concentrations are iron oxy-hydroxide and aluminum silicates, such as feldspars, amphibole, pyroxene, epidote, and micas, which is consistent with the chemical composition presented in Table 1, which shows that the most abundant elements are silicon, iron, aluminum, calcium, and magnesium.

Table 2. Minerals present in the tailing.

Mineral	Percentage	Mineral	Percentage
FeOx/Hydroxide	30.7	Pyroxene	2.3
Chalcopyrite	0.1	Epidote	3.0
Pyrite	2.6	Chlorite	6.8
Quartz	3.1	Micas	2.3
Feldspars	18.5	Apatite	3.4
Amphibole	19.9	Others	6.8

Table 3 presents the results obtained in the chemical analysis of the purified apatite sample. A high content of phosphate and lime in the sample can be observed. It was established that it is a chloroapatite sample based on its composition and from the scanning electron microscopy with an energy-dispersive X-ray spectroscopy (EDS) analysis.

Table 3. Chemical analysis of the purified apatite.

Element	CaO	P ₂ O ₅	Cl	SiO ₂	Fe ₂ O ₃	MgO	Al ₂ O ₃
(%)	37.3	37.1	3.8	2.3	1.84	0.59	0.16

According to the results shown in Tables 1 and 2, there is agreement with respect to the values obtained in the chemical analysis and the mineralogical species present in the tailings sample studied. On the other hand, Table 3 presents values that show high purity of the apatite sample used in the zeta potential and contact angle tests.

Figure 1 shows the particle size analysis results and the percentage distribution of P₂O₅ for each particle size fraction in the tailing. It is observed that 46.7% of the particles are smaller than 37 microns, and 42.2% of P₂O₅ of the total phosphate is contained under this same particle size. It is worth mentioning that the high percentage of material lower than 53 microns corresponds to 67.3%.

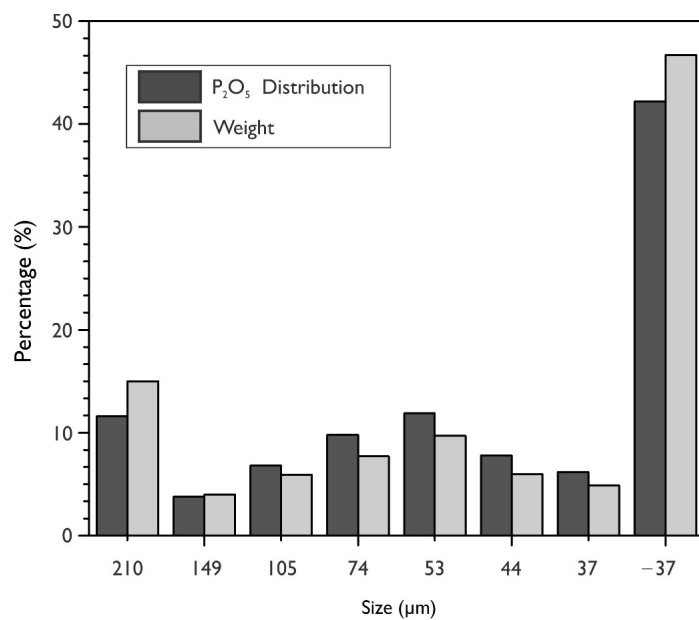


Figure 1. Particle size distribution and P_2O_5 by size.

Figure 2 shows that the contact angle without using collectors is low and presents results between 23.9° and 42.4° . However, with sodium oleate in doses of $10^{-4} \text{ mol}\cdot\text{L}^{-1}$ and $10^{-3} \text{ mol}\cdot\text{L}^{-1}$, the contact angle increases to 56.0° and 57.7° , respectively. It is also observed that the best results were obtained with Atrac-2600 throughout the pH range studied, standing out at pH 10 with a maximum angle of 63.4° . Such results are consistent with previous publications [26].

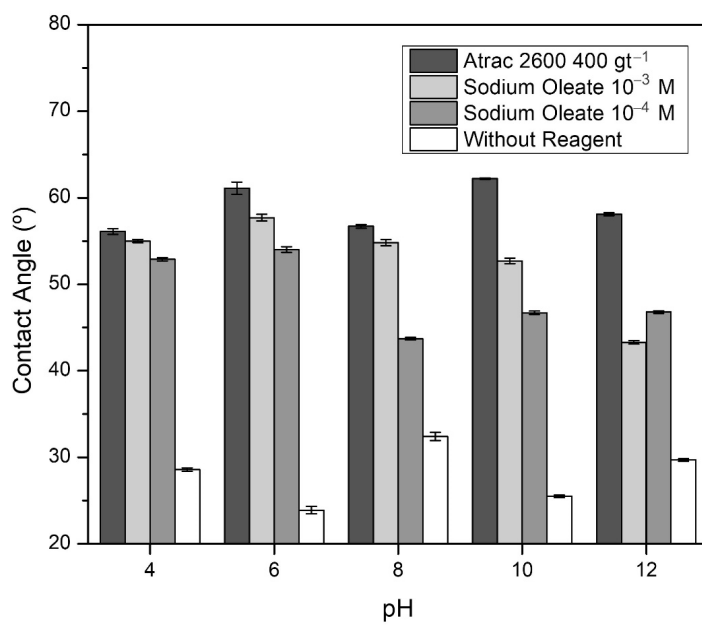


Figure 2. Contact angle as a function of pH for different collectors.

Figure 3 shows the zeta potential results as a pH function without a collector and employing sodium oleate and Atrac-2600. These tests were performed with KNO_3 as the neutral electrolyte and $NaOH$ and H_2SO_4 as the pH modifiers across a pH range of 2 to 12.

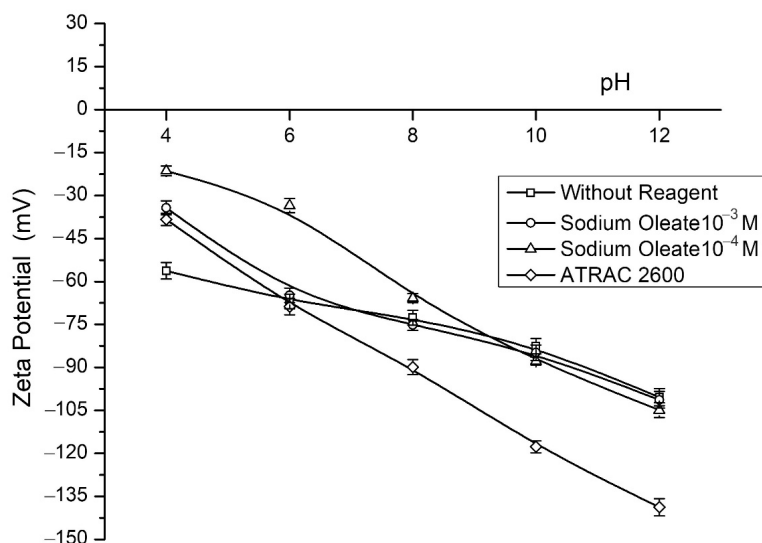


Figure 3. Results of the zeta potential at different pH values, with and without collector.

The graph illustrates that the apatite particles have a negative surface both with and without the presence of collectors. According to [27], the electrokinetic properties of apatite depend on the first-order potential-determining ions (Ca^{+2} , PO_4^{4-} , and OH^-), while H^+ ions would be the second-order potential-determining ions. The surface charges become slightly negative when applying sodium oleate in concentrations of $10^{-4} \text{ mol}\cdot\text{L}^{-1}$ and $10^{-3} \text{ mol}\cdot\text{L}^{-1}$. Using Atrac-2600, more negative zeta potentials are obtained concerning the values obtained for apatite without a collector, which would indicate adsorption of the anionic collector on the surface of the mineral despite the high repulsion that would be present at a basic pH. In this case, Atrac-2600 would be specifically adsorbed by chemisorption with apatite, hydrophobizing the surface of the mineral. Diverse researchers [27,28] have reported a high variability of the apatite isoelectric point, encountering PIE values between 2 and 8. This difference is due to the origin, composition, and substitutions, among other factors.

Several investigations on reagents used in the flotation of apatite, such as fatty acids, oleic acid, and sodium oleate, have shown through micro-flotation tests, zeta potential measurements, and XPS analysis, that the collector is chemically adsorbed on the surface of the apatite and that it is formed between the hydrogen of the fatty acid and the oxygen of PO_4 , at the surface of the apatite [29,30]. Ref. [31] correlated that it was chemisorbed by the CaO bonds' formation on the apatite surface. Also, the molecules ($\text{C}_{17}\text{H}_{33}\text{CONH}_2$) and micelles ($\text{C}_{17}\text{H}_{33}\text{CONH}_2$) with the oleic acid amide can be chemisorbed on the apatite surface by Ca-O bonds or Ca-N formation. In this study, the flotation of the apatite occurs at an alkaline pH, which suggests possible chemical adsorption of the collector, considering that at this pH, the apatite presents a negative zeta potential, which is increased by the presence of the collector, by the specific adsorption of this reagent on the surface of the mineral.

Figure 4 shows the metallurgical recovery and the P_2O_5 grade for different doses of Atrac-2600 (200, 300, 400, and 500 gt^{-1}) using 400 gt^{-1} of sodium silicate. It is observed that the recovery has a behavior directly proportional to the collector dose; namely, as the dose increases, the recovery increases as well. Similar results were stated by [32], who reported that higher doses of the synthetic collector MD 20,723 increased apatite recovery.

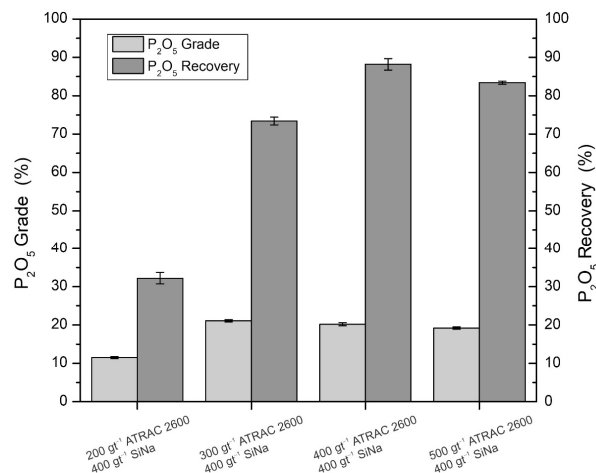


Figure 4. Effect of Atrac-2600 collector dose as a function of recovery and phosphate grade.

It is observed that the best result is obtained with a dose of 400 g t^{-1} of Atrac-2600 and 400 g t^{-1} of sodium silicate. Furthermore, a concentrate is obtained with a grade of 20.2% P_2O_5 and a recovery of 88.2%, with a high enrichment ratio of 11.2. This matter indicates a high selectivity concerning SiO_2 and Fe_2O_3 , favored by the presence of sodium silicate, whose function is the dispersion of the gangue, the increase of its hydrophilicity, and the inhibition of its flotation [33,34].

Figure 5 shows the dose effect of the methyl isobutyl carbinol (MIBC) frother agent on the metallurgical recovery and P_2O_5 grade for an Atrac-2600 dose of 400 g t^{-1} and 400 g t^{-1} of sodium silicate.

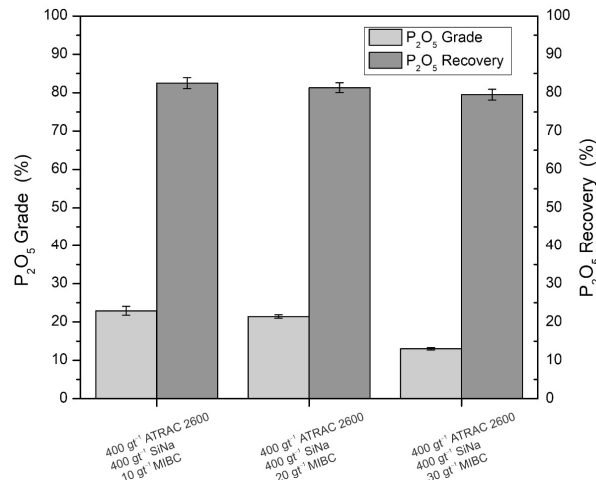


Figure 5. Effect of the frother dose as a function of grade and P_2O_5 recovery.

The figure shows that the addition of the frother decreases the recovery of P_2O_5 , and without the addition of the frother, only adding 400 g t^{-1} of Atrac-2600 and 400 g t^{-1} of sodium silicate, a recovery of 88.2% is obtained (See Figure 4). With the addition of 10 g t^{-1} of the frother, in addition to 400 g t^{-1} of Atrac-2600 and 400 g t^{-1} of sodium silicate, a recovery of 82.5% is obtained (See Figure 5). However, the P_2O_5 grade increases from 20.2% to 22.9% by adding 10 g t^{-1} of the frother. Higher doses of the frother reduce the grade and P_2O_5 recovery.

3.1. Flotation Kinetics

The results of the flotation kinetics were adjusted to the model proposed by [35]:

$$R = R_\infty \left(1 - e^{-k \cdot t}\right) \quad (1)$$

where R is the recovery (%) of valuable metal in an instant t (min), with R_∞ representing the maximum estimated recovery (%) and k is the first-order kinetic.

The kinetic parameters, confidence interval of fit at a 90% significance level (C.I.), standard error of recovery (S.E.), and correlation coefficient (R^2) obtained for each flotation stage presented in Table 4 were determined using the SOLVER function of the Microsoft Excel spreadsheet program [36].

Table 4. Kinetic parameters, confidence interval (C.I.), standard error recovery (S.E.), and correlation coefficient (R^2).

Stage	R_∞ , %	K , (min $^{-1}$)	C.I.	S.E.	R^2
Rougher	85.1	0.26	4,41	2.07	0.992
Cleaner	99.0	0.30	5.76	2.70	0.991
Scavenger	91.8	0.12	5.65	2.65	0.984

The correlation coefficient values indicate that the experimental recoveries fit the García Zúñiga model quite well, i.e., over 98.4% of the recovery variation can be explained by the variation in flotation time [35].

Table 4 also presents, as expected, that the magnitude of the kinetic constant (k) that represents the flotation speed of the particles in each stage for the cleanest stage ($k = 0.30 \text{ min}^{-1}$) is greater than for the rougher stage ($k = 0.28 \text{ min}^{-1}$), and the magnitude of the kinetic constant (k) for the rougher stage is greater than that for the scavenger stage (0.12 min^{-1}).

Figure 6 shows the accumulated recoveries as a function of time for the rougher, cleaner, and scavenger kinetics. The symbol represents the accumulated experimental recovery, while the line indicates the accumulated recovery calculated using the García Zúñiga model.

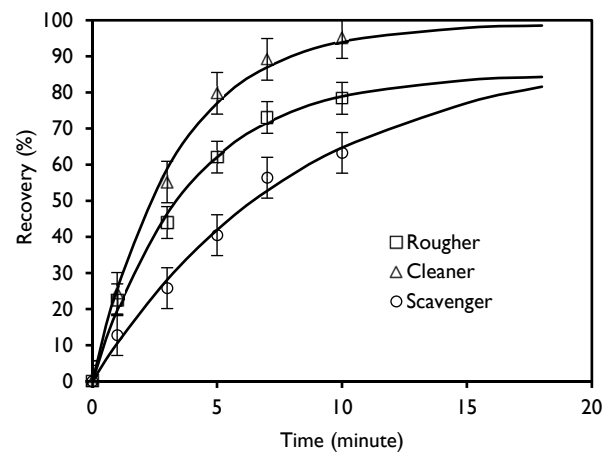


Figure 6. García Zúñiga’s kinetic model for the rougher, cleaner, and scavenger flotation stages.

It is observed that after 10 min of flotation, the recovery of apatite is 78%; however, longer times do not increase the recovery and result in a reduction in concentrate grade. The optimal flotation time for the rougher stage is established as 10 min, yielding an instantaneous and cumulative P_2O_5 grade of 5.7% and 19.5% in the concentrate, respectively. The tailing, with a 0.45% P_2O_5 grade, will undergo reprocessing in the scavenger stage. The recovery for the scavenger stage was 63.3%, and the optimum time to achieve this recovery according to the Agar criteria was 7.6 min, with P_2O_5 grades of 2.2% in the concentrate and 0.20% in the scavenger tailing. The instantaneous grade obtained for the cleaner stage was 21.7% of P_2O_5 , and the cumulative grade was 30.2% of P_2O_5 for 6.8 min.

3.2. Determination of the Split Factor

The split factor concept represents the percentage by weight of each component fed to a flotation stage that appears in the concentrate, i.e., it corresponds to the apatite and weight recoveries for the rougher, scavenger, and cleaner flotation stages. The magnitude of the split factor depends mainly on the flotation time, the physical and chemical properties of the slurry, and the mineral characteristics. Table 5 presents the split factor calculated with the open cycle tests performed with the optimal flotation time determined by flotation kinetics.

Table 5. Split factor calculated with the open cycle test.

Stage	Apatite Recovery, %	Weight Recovery, %
Rougher	6.72	77.2
Cleaner	70.47	95.3
Scavenger	15.89	62.8

3.3. Simulation of Flotation Circuits

Figure 7 shows the flotation circuit simulation using the split factor method to recover apatite from the magnetic concentration tailings of iron ore. The equations system that describes the mass balance of the flotation circuit, represented in Figure 7, was solved by the matrix inversion method using the MINVERSE and MMULT functions of Excel.

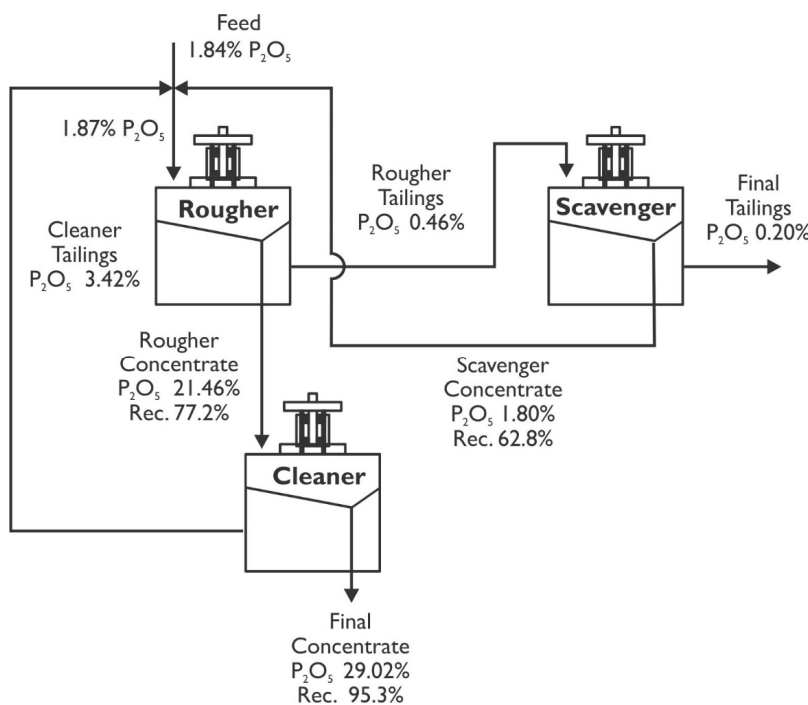


Figure 7. Flotation circuit for the apatite.

Table 6 presents the grade and recovery of P₂O₅ for each of the stages along with the global flotation circuit shown in Figure 7. The feasibility of producing concentrates with a grade of 29.1% and recovering 89.6% of the P₂O₅ contained in the iron tailings by implementing a flotation circuit comprising the rougher–scavenger–cleaner stages is observed in the table. To achieve this grade and recovery of P₂O₅, it is only necessary to condition the iron tailings with 400 g t⁻¹ of Atrac-2600, 400 g t⁻¹ of sodium silicate, a 10 min of conditioning time, pH adjustment to 10, and flotation times set at 10, 7.6, and 6.8 min for the rougher–scavenger–cleaner and recleaner stages, respectively.

Table 6. Grade and recovery of P₂O₅ for each of the stages and the global flotation circuit applying the split factor method.

Stage	Grade of P ₂ O ₅ , %			Recovery, %
	Feed	Concentrate	Tailing	
Rougher	1.87	21.46	0.46	77.2
Cleaner	21.46	29.02	3.42	95.3
Scavenger	0.46	1.80	0.20	62.8
Global flotation circuit	1.84	29.02	0.20	89.7

4. Conclusions

Based on the experimental results obtained in this study, it is concluded that:

- The utilization of the Atrac-2600 collector significantly enhanced the contact angle and hydrophobicity of the apatite. However, no adsorption of this reagent was observed on the surfaces of the gangue minerals;
- The flotation circuit must comprise the rougher–scavenger–cleaner stages to produce concentrates with P₂O₅ grades and recoveries of 29.02% and 89.7%, respectively. The iron tailings must undergo a 10 min conditioning process with 400 g t⁻¹ of Atrac-2600 collector, 400 g t⁻¹ sodium silicate dispersant, pH adjustment to 10, and flotation times for each stage set at 10, 7.6, and 6.8 min, respectively;
- The results presented in this study demonstrate that apatite can be recovered from the tailings of the magnetic concentration process of the Minera del Pacífico Company and can be a relevant source of phosphate, showing that it is feasible to transform an environmental liability into an economic resource within the mining sector, thus facilitating virtuous, inclusive, and sustainable mining.

Author Contributions: Conceptualization, L.V. and O.G.; methodology, L.V. and O.P.; software, L.V. and M.S.; investigation, L.V.; data curation, L.V. and M.S.; writing—original draft preparation, L.V.; writing—review and editing, L.V., O.G., O.P. and M.S.; visualization, L.V. and O.G.; supervision, O.P. and M.S.; project administration, O.G.; funding acquisition, L.V. and O.G. All authors have read and agreed to the publication version of the manuscript.

Funding: This study was funded by the Support Program for the Development of Applied R&D 2022 of the Faculty of Engineering of the Universidad de Atacama. Exempt Resolution No. 647, 14 July 2022.

Data Availability Statement: Data are available upon request to the authors as the ore under study is from a specific mining company; there may be restrictions in providing other data in addition to those published.

Acknowledgments: The authors would like to thank the Compañía Minera del Pacífico for donating the mineral samples for this study and the Mineral and Environmental Technology Laboratory of PPGE3M of the Federal University of Rio Grande do Sul for the chemical and mineralogical characterization of the mineral samples.

Conflicts of Interest: The authors L.V., O.P., and M.S. are professors of the Metallurgical Department of the Engineering Faculty of the Universidad de Atacama. The remaining author declares that the research was conducted in the absence of commercial or financial relationships that could be interpreted as a possible conflict of interest.

References

1. Jasinski, S.M. *Mineral Commodity Summaries*; U.S. Geological Survey: Reston, VA, USA, 2020.
2. COCHILCO—Yearbook: Copper and Other Mineral Statistics 2003–2022. Available online: https://www.cochilco.cl/Lists/Anuario/Attachments/27/ANUARIO_ESTADISTICO_COCHILCO%20A%C3%91O%202022.pdf (accessed on 15 March 2023).
3. Esposito, M.; Tse, T.; Soufani, K. Is the circular economy a new fast-expanding market? *Thunderbird Int. Bus. Rev.* **2017**, *59*, 9–14. [CrossRef]
4. Zhao, Y.; Zang, L.; Li, Z.; Qin, J. Discussion on the model of mining circular economy. *Energy Procedia* **2012**, *16*, 438–443. [CrossRef]

5. Solomons, I. Mine Tailings Recovery Can Be Value Generator. Says Council for Geoscience. *Mining Weekly*, 9 June 2017. Available online: <http://www.miningweekly.com/article/mine-tailings-recovery-can-be-value-generator-reduces-enviro-impact-2017-06-09> (accessed on 10 March 2023).
6. Castillo, C.; Ihle, C.F.; Jeldres, R.I. Chemometric Optimisation of a Copper Sulphide Tailings Flocculation Process in the Presence of Clays. *Minerals* **2019**, *9*, 582. [CrossRef]
7. Vivallo, W.; Henríquez, F.; Espinoza, S. Los depósitos de hierro del tipo magnetita-apatita: Geoquímica de las rocas volcánicas asociadas y potencialidad de la mena de hierro como fuente de mineralización de oro. *Rev. Geol. Chile* **1995**, *22*, 159–175. [CrossRef]
8. Chen, H.; Cooke, D.R.; Baker, M.J. Mesozoic iron oxide copper-gold mineralization in the central Andes and the Gondwana Supercontinent breakup. *Econ. Geol.* **2013**, *108*, 37–44. [CrossRef]
9. Brito, B.; Jerez, O.; Gutierrez, L. Incorporation of Rheological Characterization in Grinding and Tailings Slurries to Optimize the CMP Magnetic Separation Plant. *Minerals* **2021**, *11*, 386. [CrossRef]
10. Xia, W.C.; Ma, G.X.; Bu, X.N.; Peng, Y.L. Effect of particle shape on bubble-particle attachment angle and flotation behavior of glass beads and fragments. *Powder Technol.* **2018**, *338*, 168–172. [CrossRef]
11. Santos, E.P.; Dutra, A.J.B.; Oliveira, J.F. The effect of jojoba oil on the surface properties of calcite and apatite aiming at their selective flotation. *Int. J. Miner. Process.* **2015**, *143*, 34–38. [CrossRef]
12. Filippov, L.O.; Filippova, I.V.; Lafhaj, Z.; Fornasiero, D. The role of a fatty alcohol in improving calcium minerals flotation with oleate. *Colloids Surf. A* **2019**, *560*, 410–417. [CrossRef]
13. Sis, H.; Chander, S. Reagents used in the flotation of phosphate ores: A critical review. *Miner. Eng.* **2003**, *16*, 577–585. [CrossRef]
14. Jong, K.; Han, Y.; Ryom, S. Flotation mechanism of oleic acid amide on apatite. *Colloids Surf. A Physicochem. Eng. Asp.* **2017**, *523*, 127–131. [CrossRef]
15. Guimarães, R.C.; Araujo, A.C.; Peres, A.E.C. Reagents in igneous phosphate ores flotation. *Miner. Eng.* **2005**, *18*, 199–204. [CrossRef]
16. Costa, D.S.; Alves, A.S.; Budke, R.; Mendes, R.M.M.; Peres, A.E.C. Flotabilidade de apatita usando óleos vegetais da Amazônia como coletores. In Proceedings of the XXIV Encontró Nacional de Tratamento de Minérios e Metalurgia Extrativa, Salvador, Brazil, 16–19 October 2011; pp. 237–244.
17. De Oliveira, P.; Mansur, H.; Mansur, A.; Da Silva, G.; Peres, A. Apatite flotation using pataua palm tree oil as collector. *J. Mater. Res. Technol.* **2019**, *28*, 4612–4619. [CrossRef]
18. Gorochovceva, N.; Klingberg, A.; Lannefors, J. Development of anionic collectors for direct flotation of apatite from complex siliceous ores with a focus on sustainability. In Proceedings of the International Mineral Processing Congress. Proceedings: XXVII International Mineral Processing, Santiago, Chile, 20–24 October 2014; pp. 68–78.
19. Shengchao, Y.; Wei, L. Rare earth elements in the iron-oxide apatite (IOA) deposit: Insights from apatite. *Int. Geol. Rev.* **2022**, *64*, 1–18. [CrossRef]
20. Taylor, R.D.; Shah, A.K.; Walsh, G.J.; Taylor, C.D. Geochemistry and geophysics of iron oxide-apatite deposits and associated tailings piles with implications for potential rare earth element resources from historic minerals and mine tailings in the eastern Adirondack New York, USA. *Econ. Geol.* **2019**, *114*, 1569–1598. [CrossRef]
21. Birinci, M. Enrichment of Apatite-Bearing Iron Ore by Magnetic Separation and Flotation. *Eur. J. Tech. (EJT)* **2021**, *11*, 1–6. [CrossRef]
22. Pålsson, B.I.; Fredriksson, A. Apatite for extraction. II. Flotation of apatite and rare earth elements from old tailings dumps. In Proceedings of the XXVI International Mineral Processing Congress—IMPC 2012, New Delhi, India, 24–28 September 2012; ISBN 81-901714-3-7.
23. Oliveira, M.S.; Santana, R.C.; Ataíde, C.H.; Barrozo, M.A. Recovery of apatite from flotation tailings. *Sep. Purif. Technol.* **2011**, *79*, 79–84. [CrossRef]
24. Valderrama, L.; Oliva, J.; Gómez, O.; Zazzali, B. Recuperación de apatita de relaves producidos en la concentración magnética de hierro. *Rev. Holos* **2019**, *1*, 1–11. [CrossRef]
25. Atrac-2600. Available online: <https://www.nouryon.com/product/atrac-2600-anionic-surfactant-blend/> (accessed on 1 March 2023).
26. Hanumantha Rao, K.; Dwari, R.K.; Lu, S.; Vilinska, A.; Somasundaran, P. Flotation of phosphate gangue from magnetite fines—Non-ionic surfactant as Atrac collector modifier. In Proceedings of the XXV International mineral processing Congress Proceedings, Brisbane, QLD, Australia, 6–10 September 2010; pp. 1933–1943.
27. Amankonah, J.; Somasundaran, P. Effects of dissolved mineral species on the electrokinetic behavior of calcite and apatite. *Colloids Surf.* **1985**, *15*, 335–353. [CrossRef]
28. Vučinić, D.R.; Radulović, D.S.; Deušić, S.D. Electrokinetic properties of hydroxyapatite under flotation conditions. *J. Colloid Interface Sci.* **2010**, *343*, 239–245. [CrossRef]
29. Barros, L.A.F.; Ferreira, E.E.; Peres, A.E.C. Floatability of apatites and gangue minerals of an igneous phosphate ore. *Miner. Eng.* **2008**, *21*, 994–999. [CrossRef]
30. Albino, K.I.P.; Gorochovceva, N.; Klingberg, A.; Lima, O.A. New synthetic collector for the direct flotation of apatite from complex ore. In Proceedings of the XXVI Encontro Nacional de Tratamento de Minérios e Metalurgia Extrativa, Poços de Caldas, MG, Brazil, 18–22 October 2015.

31. Xie, J.; Li, X.; Mao, S.; Li, L.; Ke, B.; Zhang, Q. Effects of structure of fatty acid collectors on the adsorption of fluorapatite (001) surface: A first-principles calculations. *Appl. Surf. Sci.* **2018**, *444*, 699–709. [[CrossRef](#)]
32. Yu, J.; Ge, Y.; Hou, J. Behaviour and mechanism of collophane and dolomite separation using alkyl hydroxamic acid as a flotation collector. *Physicochem. Probl. Min. Process.* **2016**, *52*, 155–169. [[CrossRef](#)]
33. García Zúñiga, H. La recuperación por flotación es una función exponencial del tiempo. *Bol. Min. Soc. Nac. Min.* **1935**, *XLVIII*, 83–86.
34. Silva, J.; Baltar, C.; Gonzaga, R.; Peres, A.; Leite, J. Identification of sodium silicate species used as flotation depressants. *Min. Metall. Explor.* **2012**, *29*, 207. [[CrossRef](#)]
35. Qi, G.W.; Klauber, C.; Warren, L.J. Mechanism of action of sodium silicate in the flotation of apatite from hematite. *Int. J. Miner. Process.* **1993**, *39*, 251–273. [[CrossRef](#)]
36. Brown, A.M. A step-by-step guide to non-linear regression analysis of experimental data using a Microsoft Excel spreadsheet. *Comput. Methods Programs Biomed.* **2001**, *65*, 191–200. [[CrossRef](#)]

Disclaimer/Publisher's Note: The statements, opinions and data contained in all publications are solely those of the individual author(s) and contributor(s) and not of MDPI and/or the editor(s). MDPI and/or the editor(s) disclaim responsibility for any injury to people or property resulting from any ideas, methods, instructions or products referred to in the content.